Cell Calcium 80 (2019) 175–188

Contents lists available at ScienceDirect

Cell Calcium

journal homepage: www.elsevier.com/locate/ceca

Use of a microelectrode array to record extracellular pacemaker potentials from the gastrointestinal tracts of the ICR mouse and house musk shrew (*Suncus murinus*)

Julia Y.H. Liu[a,*], Peng Du[b], Wood Yee Chan[a], John A. Rudd[a]

[a] School of Biomedical Sciences, Faculty of Medicine, The Chinese University of Hong Kong, Shatin, New Territories, Hong Kong, China
[b] Auckland Bioengineering Institute, University of Auckland, New Zealand

ARTICLE INFO

Keywords:
Gastrointestinal tract
Interstitial cells of Cajal
Microelectrode array
Pacemaker potential
Slow wave

ABSTRACT

Background: The rhythmic contraction and relaxation of smooth muscles in the gastrointestinal (GI) tract is governed by pacemaker electrical potentials, also termed slow waves, which are calcium currents generated by interstitial cells of Cajal (ICCs). Malfunction of pacemaker rhythms contributes to a number of clinically challenging gastrointestinal motility disorders.

Method: A microelectrode array (MEA) was used to record slow waves in vitro from intact GI tissues freshly isolated from the ICR mouse and *Suncus murinus*. The effects of temperature, extracellular calcium and potassium concentrations on pacemaker potentials were quantified using spatiotemporal metrics.

Results: Pacemaker frequency decreased from the duodenum to the ileum in the mouse, but this phenomenon was less significant in *Suncus murinus*. In both the mouse and *Suncus murinus*, the stomach had a much lower pacemaker frequency than the intestine. Propagation velocity and amplitude were highest in the proximal intestine. Temperature significantly increased pacemaker frequency in the intestinal tissues of both species. Removal of Ca^{2+} from the medium inhibited pacemaker potential and increasing the Ca^{2+} concentration increased pacemaker frequency in the mouse ileum. Increasing K^+ concentration decreased pacemaker frequency in the absence of nifedipine.

Conclusions: The MEA allows efficient investigation of gut pacemaker frequency and propagation.

1. Introduction

Electrical pacemaking in the gastrointestinal (GI) tract is controlled by the interstitial cells of Cajal (ICCs), which can be found from the submucosal to smooth muscle layers of the GI wall [1]. A knockout study indicated that the c-kit-positive ICCs in the myenteric plexus control basal slow waves, while the ICCs from other layers may play a modulatory role [2]. A malfunction or loss of ICCs is believed to contribute to GI motility disorders, such as gastroparesis and Hirschsprung's disease [3,4].

Loss of the homeostatic control of temperature or extracellular electrolyte levels could be reasonably expected to influence GI functions. The dependence of the pacemaker frequency on temperature was previously demonstrated using a conventional microelectrode technique in the mouse small intestine [5]. Increasing extracellular K^+ (compensated with Na^+) was found to increase pacemaker frequency in the mouse proximal colon [6]. Another study using the same technique found that T-type Ca^{2+} channels in the mouse jejunum were temperature sensitive, and voltage-dependent Ca^{2+} currents in ICCs were sensitive to changes in extracellular Ca^{2+} [7].

A limitation of the conventional microelectrode recording technique is a lack of spatial information about the propagation of slow waves, which has been shown to be an important indicator of gut dysfunction [8]. Recently, the advent of in vivo high-resolution mapping using an array of spatially dense electrodes (up to 16 × 16 electrodes at 4 mm inter-electrode spacing) yielded significant insights into the role of GI dysrhythmia in disease [9–11]. A similar result was achieved in an in vitro setting with the inter-electrode spacing reduced by a factor of 20 to 0.2 mm over a 60-tipped-electrode microelectrodes array (MEA) [12–14]. The key advantages of the MEA includes the ability to strictly control the micro-environment and eliminate potential movement artefacts [15], allowing detailed measurements of slow wave propagation

Abbreviations: GI, gastrointestinal; ICCs, interstitial cells of Cajal; LMMP, longitudinal muscle myenteric plexus; MEA, microelectrode array

* Corresponding author at: 704, Lo Kwee-Seong Integrated Biomedical Sciences Building, The Chinese University of Hong Kong, Clear Water Bay Road, Hong Kong, China.
E-mail address: liuyuenhang@gmail.com (J.Y.H. Liu).

https://doi.org/10.1016/j.ceca.2019.05.002
Received 5 March 2019; Received in revised form 23 April 2019; Accepted 8 May 2019
Available online 09 May 2019
0143-4160/

to be made.

This study was designed to quantify in detail the spatiotemporal sensitivity of slow waves to temperature and extracellular Ca^{2+} and K^+ in the ICR mouse and *Suncus murinus*. Mice are commonly used in biomedical research but, unlike humans, they do not possess a motilin receptor and are also incapable of emesis. *Suncus murinus* has a motilin receptor and is used in anti-emetic drug discovery [16]. An MEA platform was used to record slow waves and developed a custom signal processing pipeline to process and interpreted slow wave data. Our new recording and signal processing techniques will enable detailed investigations of slow wave properties.

2. Materials and methods

2.1. Animals

Two-month-old outbred ICR mice (either male or female, weight 20–25 g) and adult *Suncus murinus* (either male or female, weight 50–60 g) were obtained from the Chinese University of Hong Kong. They were housed in a temperature-controlled room (24 ± 1 °C) in plastic cages (1–5 animals per cage) with artificial lighting provided between 06:00 and 18:00 h and humidity maintained at 50 ± 5%. Water and food were provided *ad libitum*. Chow (Teklad Global 19% Protein Extruded Rodent Diet, Sterilized, 2019S, Harlan, Madison, WI) was provided for the mice, and food pellets (Feline Diet 5003, PMI Feeds, St. Louis, USA) were given to the *Suncus murinus*. All experiments were conducted under animal license granted by the Government of the Hong Kong SAR with ethical approval from the Animal Experimentation Ethics Committee, The Chinese University of Hong Kong.

2.2. Solutions and drugs

All tissue manipulation and electrical recordings were performed in Krebs' solution (in mM): NaCl, 115; KCl, 4.7; KH_2PO_4, 1.2; $MgSO_4.7H_2O$, 1.2; $CaCl_2.2H_2O$, 2.5; glucose, 10; $NaHCO_3$, 25. Krebs' solutions with different concentrations of potassium ions (K^+) were prepared by compensating KCl with NaCl, while different concentrations of calcium ions were prepared by adding different amounts of calcium chloride. Nifedipine (Sigma Aldrich) was used as an L-type calcium channel blocker to eliminate movements. Stock solutions of nifedipine were prepared by dissolving the drug in dimethyl sulfoxide (DMSO). The maximum final concentration of DMSO was 0.01%, which had little effect on the mouse ileum pacemaker frequency.

2.3. Electrical recordings

The animals were euthanized using CO_2 asphyxiation. The entire GI tract was freshly isolated and placed into Krebs' medium gassed with 95% O_2/5% CO_2. A duodenal segment was taken from each mouse at least 10 mm distal to the pyloric sphincter; segments of the ileum and proximal colon were taken at least 1 cm proximal and distal to the cecum junction, respectively; the jejunal segment was taken from the middle of the whole length of the small intestine. *Suncus murinus* does not have a cecum to delineate the small and large intestine (Fig. 1A-B). Therefore, the intestine was cut into six sections of equal length and labeled from proximal to distal with sections 1,4 and 6 considered equivalent to segments from the duodenum, ileum and colon, respectively. The intact full-thickness tissue segments were incubated in gassed Krebs' medium containing nifedipine (1 μM) to reduce smooth muscle contractions (30 min for the stomach, and 15 min for other segments) before slow waves were recorded. In one experiment, after recording from the full-thickness tissues, the same tissues were used to prepare isolated mucosal layer and longitudinal muscle myenteric plexus (LMMP) layer by gently peeling off the LMMP using fine forceps under a dissecting microscope. The LMMP was then flattened onto the recording area of the MEA. Weight was added on top with two tissue anchors (a small anchor with diameter 0.5 mm followed by a large anchor with 0.8 mm diameter) to maintain contact between the tissues and the MEA.

An MEA60 chip (Ayanda Biosystems S.A.) with 3-D tip-shaped electrodes of 30 μm diameter spaced at 200 μm was used to record slow waves over an area of 1.96 mm^2. The recording platform was connected to an amplifier (MEA1060 1200x, Multichannel Systems, Germany) and signals were displayed and recorded using MC_Rack software (Multichannel Systems, Germany). Temperature was controlled by a software-controlled heated copper plate underneath the recording chamber and was maintained at 35.0 °C unless stated otherwise. The whole set-up was shielded from environmental noise using a Faraday cage (Fig. 1C). The whole stomach was then placed onto the ~1 mm^2 MEA recording field with the muscular side of the corpus and antrum directly facing the electrodes. The intestinal segments were also placed directly onto the electrodes with the lumen aligned horizontally across the electrode field (Fig. 1D). An aluminum tissue anchor (ALA Scientific Instruments) was placed on top of the tissue samples to increase contact between the tissue and the electrodes. Pacemaker potentials were recorded at a sampling frequency of 1 kHz.

2.4. Organ bath

Gut tissues were harvested using procedures similar to those described in Section 2.3. Segments approximately 15 mm long were mounted under 0.5–1 g tension in a 10 ml organ chamber maintained at 35 °C. The chamber was constantly perfused with fresh warmed Kreb's solution and gassed with 95% O_2/5% CO_2. Tension changes were recorded using an isometric force displacement transducer (Grass Instruments, Inc., Quincy, MA, USA), amplified and digitalized using an analog-to-digital converter (Model ML870, PowerLab 8/30, AD Instruments), and displayed and saved using LabChart 7 software (AD Instruments). The sampling frequency was 1 kHz. Tissues were stabilized for 20 min before the addition of 120 mM potassium chloride for 0.5–1 min to provide a reference response to normalize further data. The tissue samples were washed and stabilized for another 20 min before drug treatments.

2.5. Immunofluorescence staining

The mouse ileum was dissected and cut along the longitudinal axis to expose the mucosa. The mucosa was then carefully removed by rubbing with a cotton swab. The remaining longitudinal muscle myenteric plexus (LMMP) layer was fixed with 4% paraformaldehyde in phosphate buffered saline (PBS) for 2 h and then washed with PBS. The LMMP layer was permeabilized with 0.25% Triton X-100 in PBS for 1 h, followed by blocking and nuclei staining with DAPI Nucleic Acid Stain (1:5000, Thermo Fisher) diluted in 3% bovine serum albumin (BSA) in 0.25% Triton X-100 in PBS for another 1 h. The tissue samples were then incubated with primary antibodies CD117 (c-kit) (1:100, Dako) diluted in 3% BSA in 0.25% Triton X-100 in PBS overnight at 4 °C. The following day, the tissue samples were washed with PBS three times, and incubated with secondary sheep anti-rabbit IgG (H + L) antibodies and tetramethylrhodamine (TRITC) conjugate (1:500, Thermo Fisher) diluted in 3% BSA in 0.25% Triton X-100 in PBS for 2 h at room temperature. The samples were then washed with PBS three times and mounted on microscope slides. An Olympus confocal microscope (model FV1200) was used for photo capture and an auto-calibrated scale bar was introduced using FV10-ASW 1.7 Viewer software (Olympus).

2.6. Temporal data analysis and statistics

Raw data from the MEA and the organ bath were imported into Spike 2 (version 8.0, Cambridge Electronic Design Limited) for analysis.

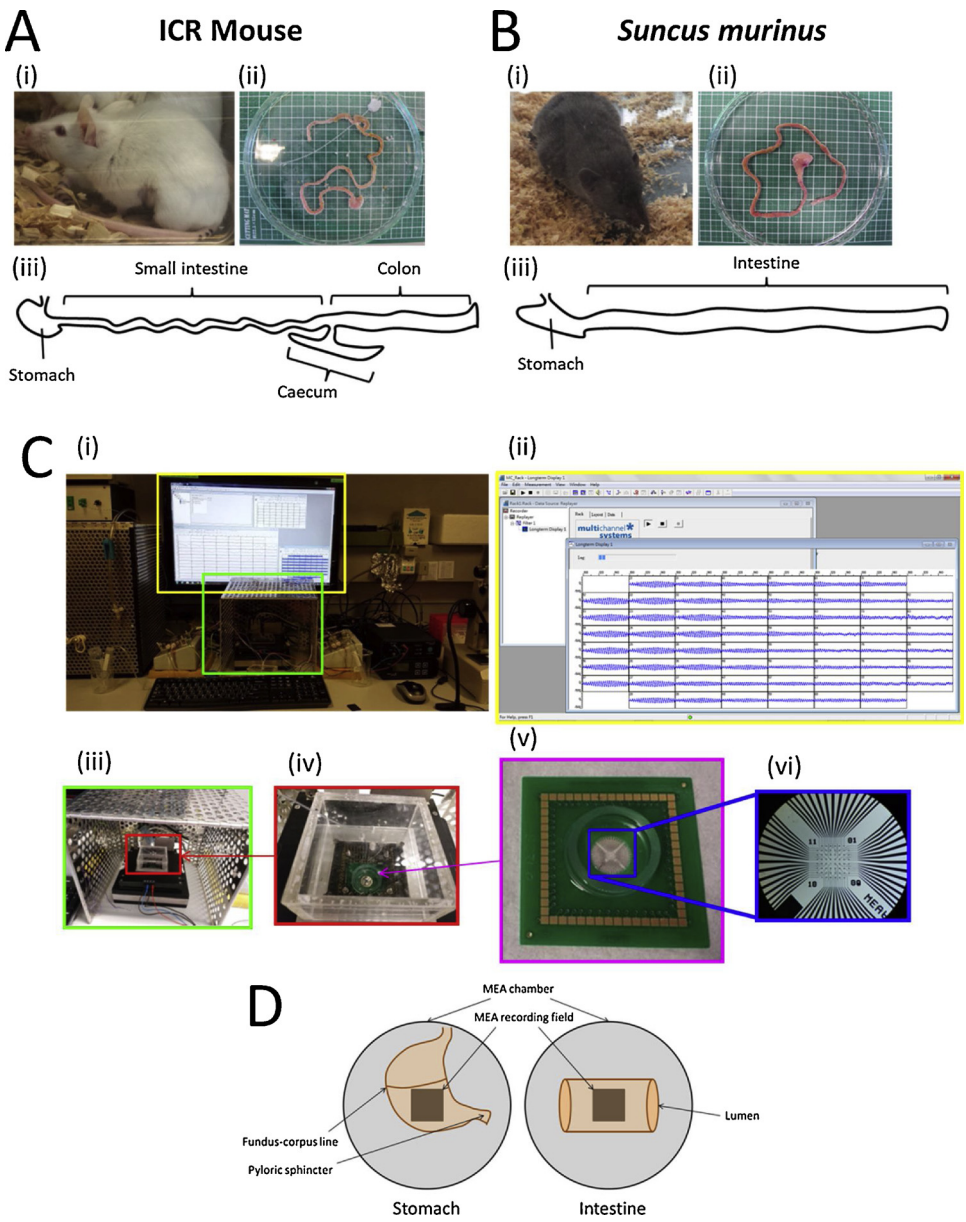

Fig. 1. Experimental set-up. The structure of the gastrointestinal (GI) tract of **(A)** ICR mouse and **(B)** *Suncus murinus*. **(i)** Representative photographs of the species; **(ii)** representative photographs of freshly isolated GI tracts (with fat and connective tissues removed) taken on a 1 cm^2 scaled mat; **(iii)** drawings of the GI structures. **(C)** The microelectrode array (MEA) system. **(i)** The general organization of the MEA set-up; **(ii)** MC_Rack software (Multichannel Systems, Germany) was used for raw data recording; **(iii-iv)** the recording platform was installed inside a Faraday cage with an MEA-chip inserted into a recording chamber with a transparent lid and temperature adjusted by a software-controlled copper plate underneath the chamber; **(v-vi)** the MEA60 chip, designed by Ayanda Biosystems S.A., Switzerland with 60 3D electrodes, 8 × 8 array (no electrodes in the corners), inter-electrode spacing at 200 µm. **(D)** Orientation of the stomach and intestinal tissues for all recordings of pacemaker potential.

A second-order Butterworth lowpass IIR filter with a cutoff of 100 Hz was applied to the raw data, which was then down-sampled to 100 Hz. A bandpass with a cutoff interval of 0.05–0.5 Hz was then applied to the down-sampled data. Dominant frequency of the filtered data was calculated using FFT analysis. The pacemaker frequencies are expressed in cycle per minute (cpm). Statistical analysis was performed using one-way ANOVA followed by Tukey's multiple comparison tests using Graphpad PRISM 5.0 software. All numerical data were expressed as mean ± S.E.M. and a p-value of < 0.05 was considered statistically significant. The number of animals (n) used for each experiment is specified in the figure legends and in the result section. The smooth muscles contractions were measured in gram (g) and pacemaker potentials were measured in microvolt (µV).

2.7. Spatiotemporal analysis of MEA data

The MEA data were processed based on a combination of published MATLAB methods [17,18]. The raw data were filtered using a third-order Savitzky-Golay filter without any down-sampling based the following equation:

$$f_c = \frac{N+1}{3.2M - 4.6} \quad (1)$$

where f_c is the normalized cut-off frequency, N is the order of the filter (N = 3), and M is the half-width (M = 901). Based on the parameters used in Eq. (1) and a sampling frequency of 1 kHz, the effective digital cut-off frequency was approximately 1.4 Hz.

A positive amplitude-sensitive differentiator (ASD) transform was applied to the intestinal and colonic slow wave signals [19]. A falling-edge negative gradient approach was not adopted due to the monophasic signal morphology in which the upstroke was more identifiable than the downstroke in the intestinal signals (Fig. 2). The equation for the ASD transform was

$$ASD\ [V_n] = \left| V_n \times \frac{dV_n}{dt} \right| \quad (2)$$

where V_n is the n^{th} sample in a single channel, and dV_n/dt is the first-order derivative of the signal, with all of the negative values set to 0 V/s. The inverse of the gastric slow wave recordings was used to identify the point of steepest negative gradient. The result of the transform was a series of pulses corresponding to the point of steepest positive

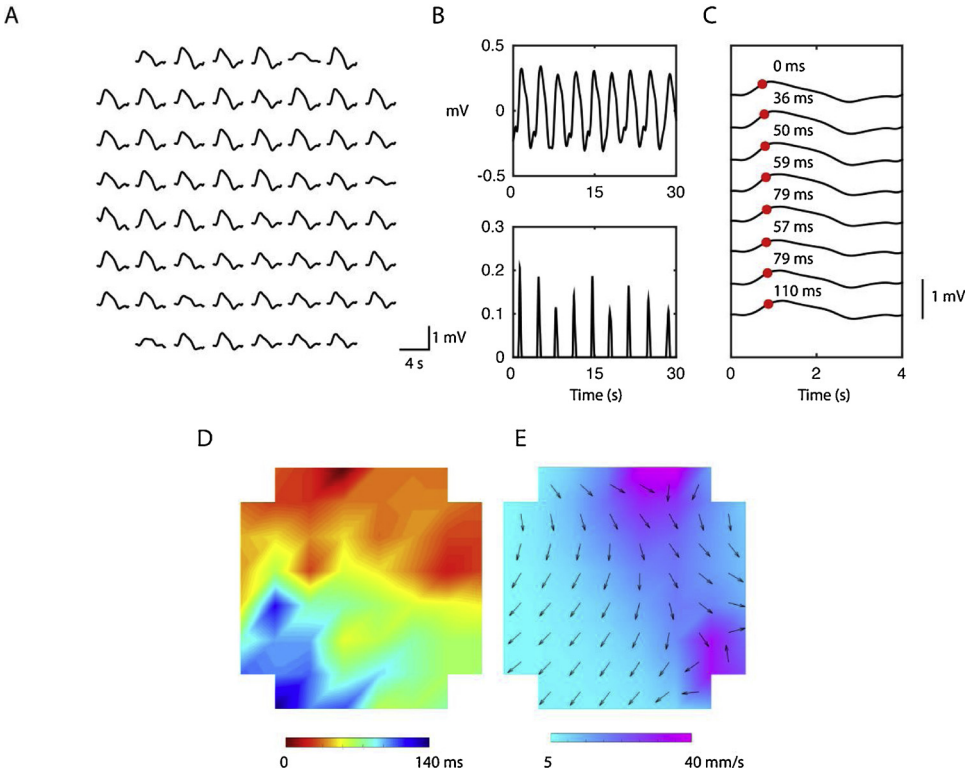

Fig. 2. Analysis of MEA data. (A) A single cycle of slow wave signals recorded by the MEA; **(B)** an example of a slow wave signal trace (top) and the signal transformed using Eq. (2)(bottom); **(C)** identified activation times are marked as red dots with the lag times labelled; **(D)** activation times map; **(E)** velocity map.

deflection in the slow wave. The peaks of the ASD were identified and grouped into individual cycles based on a ratio of the average interval. This threshold was mostly set to 0.1 of the average of intervals, which were approximately 10–15 s for gastric slow waves, and 1.2–2 s for the intestinal slow waves.

Velocity was calculated based on the method proposed in [20] by fitting a second-order polynomial to the activation times map and then calculating the velocity vector at each electrode using the following equation:

$$\begin{bmatrix} \frac{dx}{dt} \\ \frac{dy}{dt} \end{bmatrix} = \begin{bmatrix} \frac{T_x}{T_x^2 + T_y^2} \\ \frac{T_y}{T_x^2 + T_y^2} \end{bmatrix} \quad (3)$$

where T_x and T_y are the derivatives with respect to the x- and y- directions, respectively. In addition to velocity, the amplitudes of the slow waves were measured as the absolute difference between the maximum and minimum within 600 ms of the activation times.

3. Results

3.1. Pacemaker frequency of different tissue sections along the GI tract

In both the mouse (n = 4–6) and *Suncus murinus* (n = 4–6), the antral pacemaker frequency was significantly lower than that of the intestine ($p < 0.001$) (Fig. 3). At 35.0 °C, the pacemaker frequencies of the mouse gastric corpus, duodenum, jejunum and ileum were 6.5 ± 0.4 cpm, 26.6 ± 1.5 cpm, 22.6 ± 1.1 cpm and 21.8 ± 0.9 cpm, respectively; the pacemaker frequencies of the *Suncus murinus* gastric antrum, intestinal sections 1,4 and 6 were 6.7 ± 0.7 cpm, 26.3 ± 1.3 cpm, 26.5 ± 1.2 cpm and 24.4 ± 1.2 cpm, respectively measured by the MEA.

The success rate of recording reliable pacemaker potentials by the MEA was low (< 5%) in the mouse colons, compared to a rate of almost 100% for recording small intestinal pacemaker signals, and a rate of 50–60% for recording gastric pacemaker signals. The few successful records of pacemaker potentials in the mouse colon were from only a few MEA channels. However, this was not the case for *Suncus murinus*, which does not have a defined cecum as a clear boundary between the ileum and the colon. Intestinal sections 5 and 6, which approximated the colon, expressed pacemaker potentials similar to those of the small intestinal sections 1–4.

3.2. Temperature dependence of pacemaker frequency

The frequency of slow waves increased between 30 °C and 40 °C in all intestinal segments in both species ($p < 0.05$, n = 4–6) (Fig. 4). In the stomach of the mouse, the pacemaker frequency significantly increased between 35 °C and 40 °C, while pacemaker potentials were weak and unstable below 35 °C. However, this temperature dependence was not observed in the gastric antrum of *Suncus murinus* ($p > 0.05$).

3.3. The proximal intestinal segment produced the highest amplitude, frequency and propagating velocity

The spatiotemporal characteristics of pacemaker potentials demonstrated similar dependence on temperature as the frequency analysis (Fig. 5). Furthermore, the propagation velocity and amplitude were identified in the different gut segments. At 35 °C, the propagation velocities in the *Suncus murinus* antrum and intestinal sections 1,4 and 6 were 2.2 ± 0.6 mm/s, 7.6 ± 3.7 mm/s, 2.8 ± 0.8 mm/s and 1.5 ± 0.3 mm/s, respectively (n = 4–6). In general, the frequency, amplitude and velocity of slow waves were higher in the intestine compared to the antrum, with the proximal intestine segments produced the highest of all three measurements. The velocity of slow waves in section 6 was similar to that of the gastric slow waves, even though the frequency and amplitude of the slow waves in section 6 were higher than those of the gastric slow waves. In general, the frequency

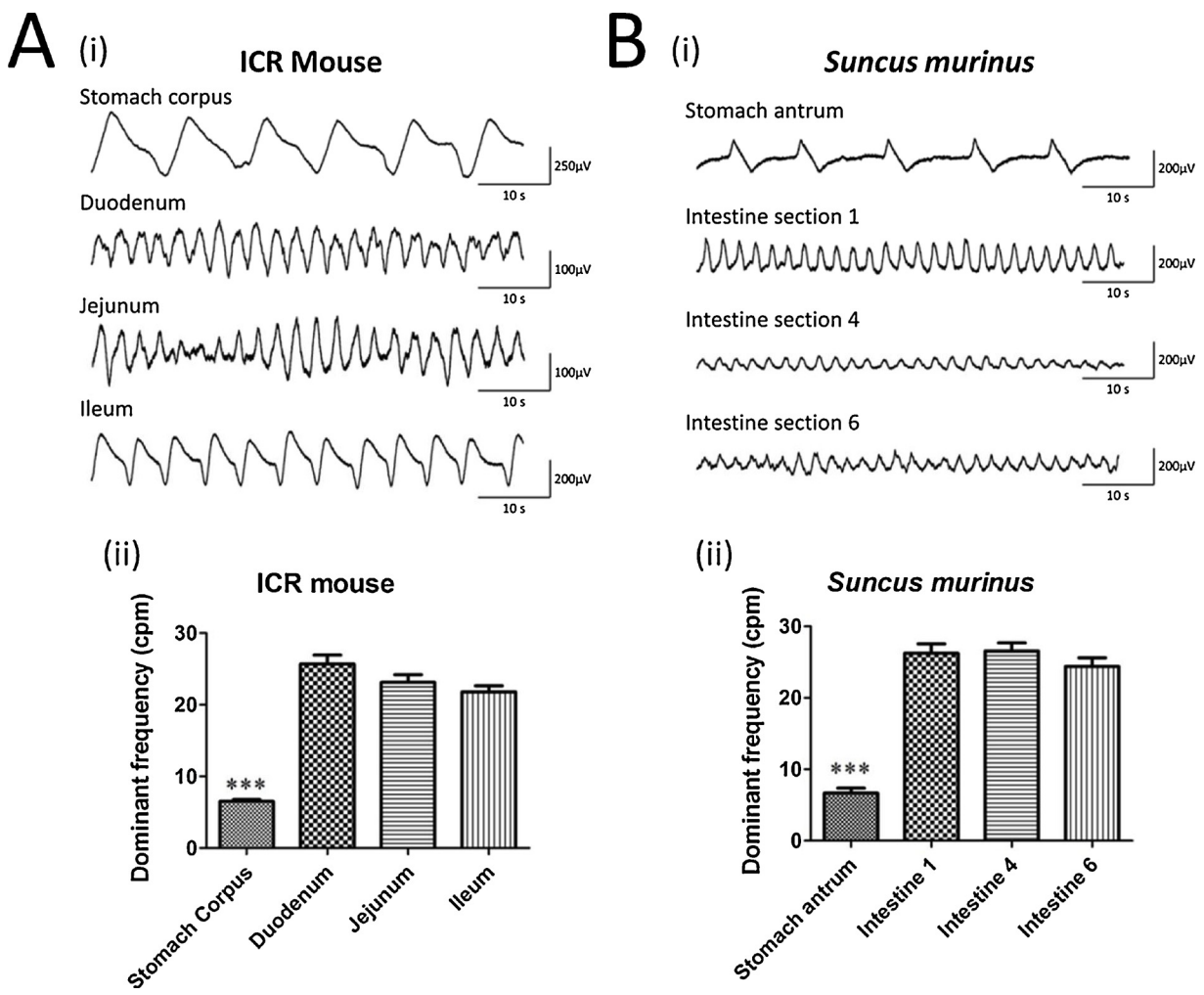

Fig. 3. Regional differences in the pacemaker frequencies in the GI tracts of the mouse and *Suncus murinus*. **(i)** Representative raw traces of pacemaker potentials recorded using the MEA in different GI sections in **(A)** the ICR mouse and; **(B)** *Suncus murinus*; **(ii)** data are the mean ± S.E.M. of 4–6 determinations. Significant differences relative to the stomach are indicated as *** $p < 0.001$ (one-way ANOVA followed by Tukey's multiple comparison tests).

increased while both amplitude and velocity decreased as the temperature increased in all segments. The rates of change of the frequency, amplitude and velocity of pacemaker potentials due to temperature are listed in Table 1. It is notable that the effects of temperature were greater on amplitude and frequency than the natural gradients while the opposite was true for velocity (Fig. 5). The frequency data derived from the conventional Butterworth filtering method matched to those derived from the spatial-temporal analysis using the Savitzky-Golay filtering method. The analysis of data from the mouse tissues showed temperature-dependent frequency comparable to that seen in the tissues from *Suncus murinus*. However, in the mouse, the peak amplitude appeared at 35 °C, and the velocity was highest at the jejunum.

Examples of slow waves and activation maps from each segment are shown in (Fig. 6). The propagation direction with respect to the entire GI tract could not be established in the isolated segments, but it is most likely that the most common propagation direction was antegrade. The figure also shows two instances when the propagation spontaneously changed direction in the same segment at different temperatures. The prevalence of spontaneous changes in direction was low. At 35 °C in section 4, the propagation showed an uncoupling behavior where the slow waves in the right part of the array occurred with a noticeable lag of ~1.1 s compared to the left part of the array (Fig. 6C,E). The frequencies of the two regions were identical (~26 cpm; $p > 0.05$). At 37.5 °C the propagation in section 6 switched direction compared to the direction at 30 °C (Fig. 6D,F), probably from antegrade propagation to circumferential propagation, as the velocity was notably increased (7.2 ± 4.1 vs 4.9 ± 3.3 mm/s; $p < 0.003$) even with an elevated frequency (20 vs 16 cpm).

3.4. Effects of extracellular potassium ion concentration on pacemaker frequency

In the mouse, decreasing $[K^+]_o$ from 6 mM (standard) to 2 mM, or increasing it to 12 mM, did not affect pacemaker frequency ($p > 0.05$, n = 6–8) (Fig. 7A(i)). At 24 mM $[K^+]_o$, the pacemaker potentials were inhibited. A previous study using mouse tissues indicated that nifedipine masks the effects of $[K^+]_o$ [6]. Therefore, nifedipine (1 μM) were excluded in this specific analysis. Without nifedipine, reducing $[K^+]_o$ from 6 mM to 2 mM significantly increased the pacemaker frequency in the mouse ileum at 35.0 °C ($p < 0.05$, n = 6–8), while increasing $[K^+]_o$ to 12 or 24 mM gradually inhibited the pacemaker potential and reduced pacemaker frequency (Fig. 7A(ii)-(iii)). The pacemaker frequencies were 21.4 ± 0.4 cpm, 19.9 ± 0.5 cpm, 18.6 ± 0.6 cpm and 18.6 ± 0.2 cpm at 2, 6, 12 and 24 mM $[K^+]_o$, respectively (n = 6–8).

Without blocking L-type calcium channels with nifedipine, KCl (120 mM) induced smooth muscle contraction. This masked the spontaneous pacemaker contractions in the organ bath, which were recovered by washing with fresh Kreb's solution (Fig. 7A(iv)).

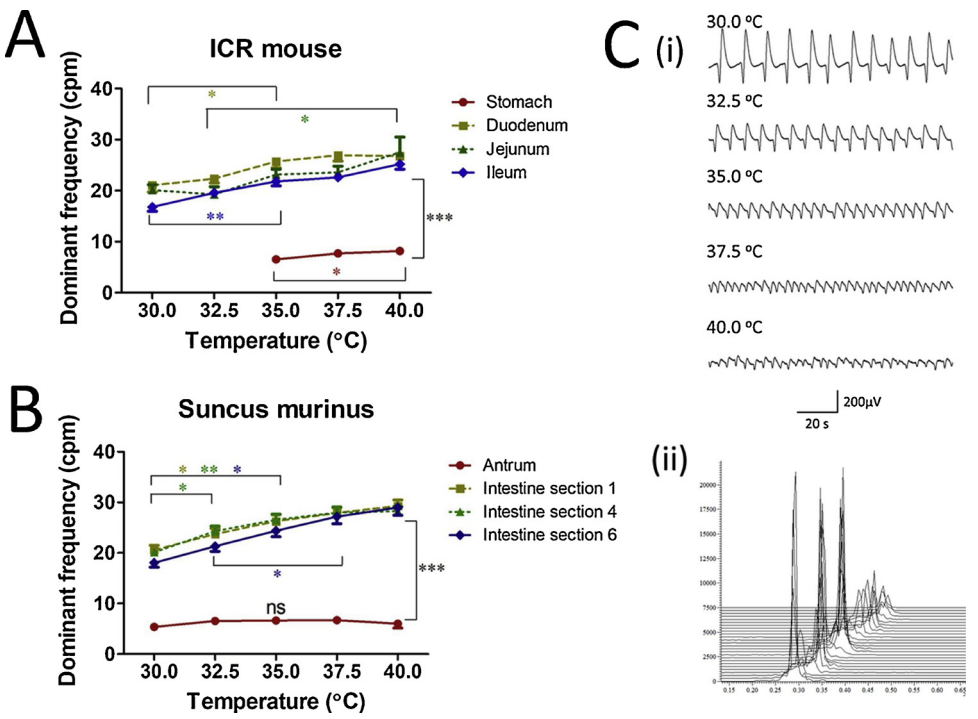

Fig. 4. The effect of temperature on pacemaker frequency in different sections of the GI tract of (A) the mouse and (B) *Suncus murinus*. Data are the mean ± S.E.M. of 4–6 determinations. Significant differences between temperatures are indicated as * $p < 0.05$, ** $p < 0.01$ and *** $p < 0.001$ (one-way ANOVA followed by Tukey's multiple comparison tests). Only significant differences in the minimum temperature range are shown; **(C)** (i) representative raw traces of pacemaker potentials in the mouse ileum from 30 °C to 40 °C (ii) representative running power spectrum with y-axis intensity in counts and x-axis frequency in Hz. Each line represents 4 min data with 75% overlapping i.e. 1 min interval between each line.

3.5. Effects of extracellular calcium ion concentration on pacemaker frequency

Pacemaker potentials generated from ICCs are calcium ion currents [21]. Perfusion of the ileum with Kreb's solution lacking calcium ions significantly inhibited pacemaker potential, which was recovered by perfusing with standard Kreb's solution (Fig. 7B(i)). Reducing $[Ca^{2+}]_o$ concentration from 2.5 mM (standard) to 1 mM did not affect pacemaker frequency in the mouse ileum at 35.0 °C ($p > 0.05$, n = 5–6). However, increasing $[Ca^{2+}]_o$ to 10 or 20 mM significantly increased pacemaker frequency ($p < 0.01$) (Fig. 7B(ii)-(iii)) from 20.3 ± 0.6 cpm, to 22.7 ± 0.6 cpm and 24.6 ± 0.7 cpm for 2.5, 10 and 20 mM $[Ca^{2+}]_o$, respectively (n = 5–6).

3.6. Variety of pacemaker potential waveforms observed using the MEA

A variety of waveforms were recorded from the MEA. Selected unfiltered traces from the mouse ileum are shown in Fig. 8A. The scales of the MEA electrodes were aligned with the immunofluorescence stained ICC networks. The field pacemaker potentials recorded from one electrode are likely to have come from several ICCs surrounding the electrode (Fig. 8B). In some cases, all 60 channels of the MEA simultaneously showed raw recordings with similar amplitudes and frequencies, indicating synchronization (Fig. 8C). In other cases, resonance of amplitudes was identified, indicating waxing and waning and modulatory effects of pacemaker potentials (Fig. 8D), which was often seen in the *ex vivo* organ bath.

3.7. Comparing pacemaker potentials recorded in the MEA to smooth muscle spontaneous contraction in the organ bath

Spontaneous smooth muscle contractions were recorded in the *ex vivo* organ bath study. The stomachs of both the mouse (n = 6–10) and *Suncus murinus* (n = 5–6) expressed a significantly lower spontaneous contraction frequency than the intestine (Fig. 9A, 9C-E). The pacemaker frequencies of the mouse stomach, duodenum, ileum and proximal colon were 6.1 ± 0.2 cpm, 36.5 ± 1.2 cpm, 24.3 ± 0.4 cpm and 10.9 ± 2.7 cpm at 35 °C respectively; the pacemaker frequencies of the *Suncus murinus* stomach, intestinal section 1,3,4 and 6 were 11.9 ± 1.1 cpm, 33.9 ± 2.8 cpm, 27.8 ± 2.3 cpm and 29.0 ± 2.0 cpm and 29.3 ± 1.8 cpm at 35 °C, respectively (Fig. 9D-E). In the proximal colon of the mouse, although the same section (1 cm distal to the cecum) was used in all experiments, the spontaneous contractions showed a variety of waveforms and patterns. In some cases, a migrating myoelectric complex could be seen (Fig. 9B). This was different from the *Suncus murinus* samples, in which the colon sections 5 and 6 expressed similar spontaneous contraction patterns to the small intestinal sections 1 and 4.

3.8. Comparing the pacemaker potentials recorded from full-thickness intestinal tissues to isolated mucosal or longitudinal muscles myenteric plexus layers

The effects of removing the mucosal layer or isolating the LMMP layer were also tested to approximate the preparation reported in a number of conventional microelectrode studies [6,12–14,22]. However, this procedure severely disrupted the signals generated by ICCs and recorded by the MEA in our experiment (Fig. 10). Pacemaker potentials signals recorded from either the tissues with the mucosal layer removed or with LMMP layers removed demonstrated irregular waveforms compared with the regular potentials recorded from the full-thickness preparations of the same intestinal tissues.

4. Discussion

A detailed account of the pacemaker potentials using isolated GI tissues from the stomach, duodenum, jejunum and ileum of the mouse; and from the stomach antrum and the whole intestine from *Suncus murinus*, using an MEA recording technique were reported. The properties of the pacemaker potentials, including differences between tissue sections and temperature dependence were consistent with published studies [5]. In addition, an analysis pipeline was developed to determine the wave amplitude and velocity across the MEA. The main findings were that the fastest propagation velocity appeared at the proximal intestinal section compared to the stomach and the rest of the intestine in *Suncus murinus*, but at the medial intestinal section in the

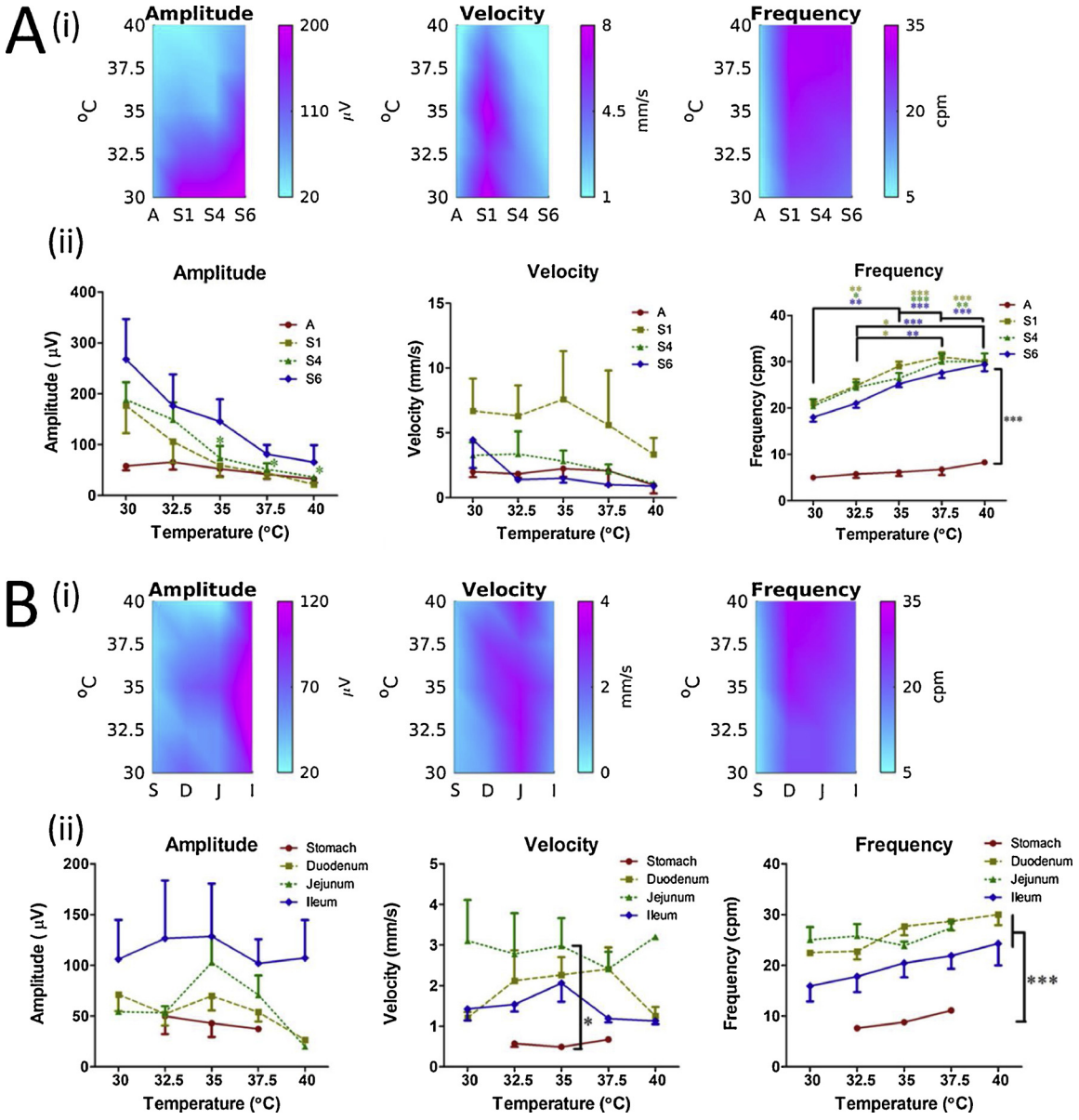

Fig. 5. The effect of temperature on pacemaker frequency, amplitude and propagation velocity in different sections of the GI tract of (A) the *Suncus murinus* and (B) the mouse. (i) spatial variations of slow waves and dependence of slow wave characteristics on temperature in terms of amplitude, velocity and frequency; (ii) statistical analysis using data derived from MATLAB spatiotemporal analysis. Significant differences between temperatures are indicated as * $p < 0.05$, ** $p < 0.01$, *** $p < 0.001$ (one-way ANOVA followed by Tukey's multiple comparison tests). **A**: Antrum of the stomach; **S1**: proximal intestine (duodenum); **S4**: middle intestine (ileum); **S6**: distal intestine (colon) in the *Suncus murinus* and **S**: stomach; **D**: duodenum; J: jejunum; **I**: ileum in the mouse.

Table 1
Rates of change in pacemaker potential characteristics due to temperature in mouse and *Suncus murinus* tissue samples.

	Frequency (cpm/°C)	Amplitude (μV/°C)	Velocity (mm/s/°C)
Mouse			
Corpus	0.5 ± 0.3	−7.9 ± 8.5	−0.1 ± 0.1
Duodenum	0.8 ± 0.5	−8.0 ± 5.7	−0.2 ± 0.2
Jejunum	1.3 ± 0.7	−21.0 ± 12.8	−0.4 ± 0.4
Ileum	1.2 ± 0.7	−5.7 ± 4.0	−0.1 ± 0.1
Suncus murinus			
Antrum	0.3 ± 0.1	−3.7 ± 3.6	−0.2 ± 0.1
Section 1	0.9 ± 0.2	−16.2 ± 11.9	−0.9 ± 0.8
Section 4	1.0 ± 0.6	−18.3 ± 9.8	−0.2 ± 0.2
Section 6	1.1 ± 0.4	−20.2 ± 13.9	−0.3 ± 0.3

mouse. The propagation direction was mostly antegrade (i.e., parallel to the lumen), but some circumferential propagation was also observed.

4.1. Ion dependence of pacemaker potential

The electrolyte dependence properties we observed differed from previously published findings. A previous investigation that used a conventional microelectrode technique to study the intracellular membrane potentials from a single ICC found that increasing $[K^+]_o$ from 5.9–20.0 mM increased pacemaker frequency [6]. The opposite was observed in the present study: increasing $[K^+]_o$ from 6 to 24 mM reduced the frequency and eventually inhibited pacemaker potential, while reducing $[K^+]_o$ from 6 to 2 mM significantly increased in pacemaker frequency (Fig. 7A). The major differences between the previous study by Hotta and colleagues and the present study are that the previous study recorded intracellular membrane potentials from the

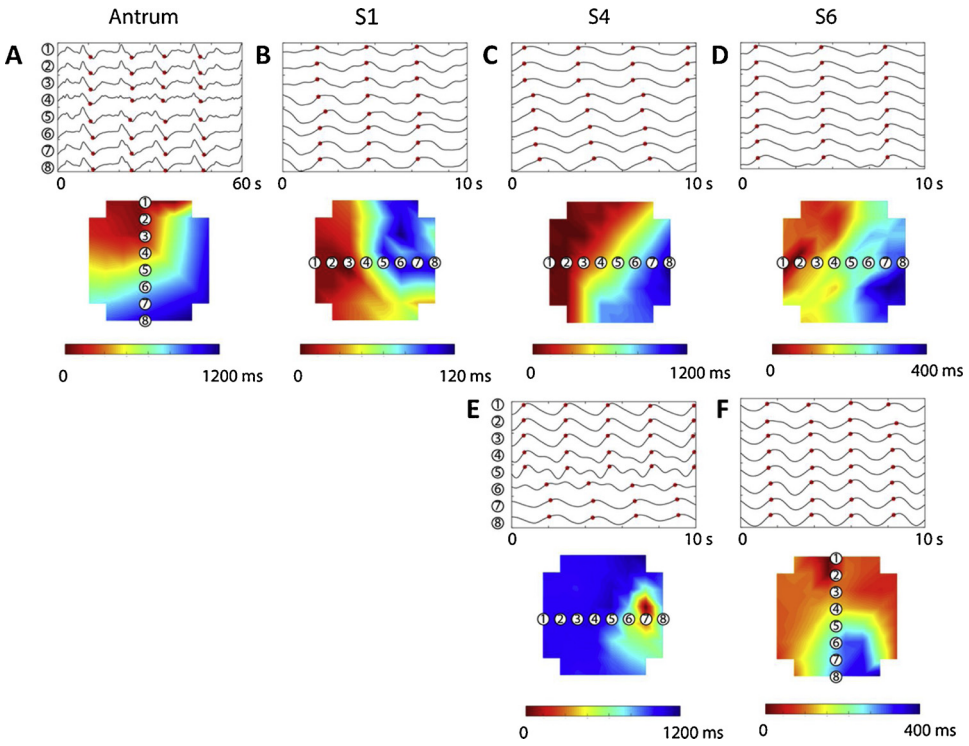

Fig. 6. Activation times maps of slow waves. **(A-D)** Examples of baseline pacemaker potentials in different segments of the gastrointestinal tract. **A**: Antrum; **S1**: proximal intestine (duodenum); **S4**: middle intestine (ileum); **S6**: distal intestine (colon); **(E-F)** two examples of spontaneous change in slow wave propagation; (E) shows uncoupled slow wave propagation and (F) shows likely circumferential propagation with an associated increase in frequency.

proximal colon [6], whereas the present study recorded extracellular potentials from the ileum. Indeed, it is worth noting the different responses of the ileum and colon to the same treatment, which may highlight potential differences in physiology and receptor expressions. Other studies have also reported opposite effects under the same treatment between the duodenum and colon [23–25]. Unfortunately, we were unable to confirm the findings in the mouse colon using the MEA. Another possible reason for the discrepancies could be arise from using different methods to dissect the tissue preparations. Thus, the removal of the mucosal layer by Hotta and co-workers is likely significantly impacted on the scope and quality of recordings. It is unknown whether the depolarizations of the mucosal layer contribute to the final results in a full-thickness preparation, but the preparation may considered to be more intact, and therefore, more representative of the physiological situation. Another factor that may contribute to discrepancies is the time-course of treatments used between the studies. The current studies focused on the acute effects of treatments, usually within 5–6 min. In the organ bath, a contraction could usually be observed upon high $[K^+]_o$, followed by a slightly overshooting relaxation response, which slowly returned back to normal contraction state upon washing (Fig. 7A(iv)).

Physiologically, increasing the $[K^+]_o$ depolarizes the ICC cell membrane, which subsequently activates the voltage-dependent Ca^{2+} channels, including T-type Ca^{2+} channels and partly L-type Ca^{2+} channels. The increase in $[Ca^{2+}]_i$ further activates the Ca^{2+} -activated Cl^- channels in ICC cells [26]. Therefore, increasing the $[K^+]_o$ may keep the cell under a pre-depolarization state. In our experiment, we also lowered $[K^+]_o$ and found that frequencies were increased, which may be explained by a higher concentration gradient across the cell membrane, including the compensating higher $[Na^+]_o$. Faster movements of K^+ and Na^+ may partly contribute to an increase in frequencies of slow wave events by inducing a steeper depolarization slope. Further studies with careful design may be required to understand the discrepancies in the response to $[K^+]_o$ between the colon and ileum in the mouse.

However, one important finding that was consistent between the two studies was that the effect of changing the $[K^+]_o$ on pacemaker potential was blocked by nifedipine. Increasing $[K^+]_o$ induce contraction which had masked the pattern of spontaneous smooth muscle contractions. It is possible that the smooth muscle might have participated in regulating the effects of $[K^+]_o$ and influenced the electrical field potentials generated by the ICCs.

In addition to studying the effects of $[K^+]_o$ on pacemaker frequency, we investigated the effects of $[Ca^{2+}]_o$. Interestingly, we found that pacemaker frequency was significantly increased when $[Ca^{2+}]_o$ increased from 2.5–20 mM, while reducing it to 1 mM had no effect, but further reducing it to 0 mM abolished pacemaker potentials (Fig. 7B). The effect of abolishing pacemaker potentials was expected [21]. The effects of $[Ca^{2+}]_o$ on pacemaker potentials appear to be independent of the smooth muscle, as our experiments were performed in the presence of nifedipine. This observation may be explained by the higher concentration gradient increasing the rate of calcium ion influx across the cell membrane when the ion channels open, increasing the frequency of the pacemaker potential. In addition, an increase in $[K^+]_o$ and $[Ca^{2+}]_o$ changes the Nernst potentials associated with each ion species and thereby changes the kinetics of the channels associated with each ion [27].

4.2. Suncus murinus may be a better model to use when studying pacemaker potentials using the microelectrode array

The major differences in the pacemaker potentials obtained from MEA recordings of the mouse and *Suncus murinus* tissues included (1) recording was challenging from the colon of the mouse but not from *Suncus murinus*, and (2) pacemaker potentials were generally more regular and with higher in amplitudes using tissues from *Suncus murinus* compared with mouse tissues. It was interesting to observe that pacemaker potentials from the mouse colon were only recorded from a few channels on the MEA. As estimated by the inter-electrode distance, the area of these few channels was approximately 0.04 mm^2 to 0.36 mm^2. This was different from the result obtained from the intestine and stomach samples, for which all 60 electrodes usually showed similar synchronized traces. It is believed that cells located at a specific region were contributing to pacemaker activity in the colon (Fig. 8). The

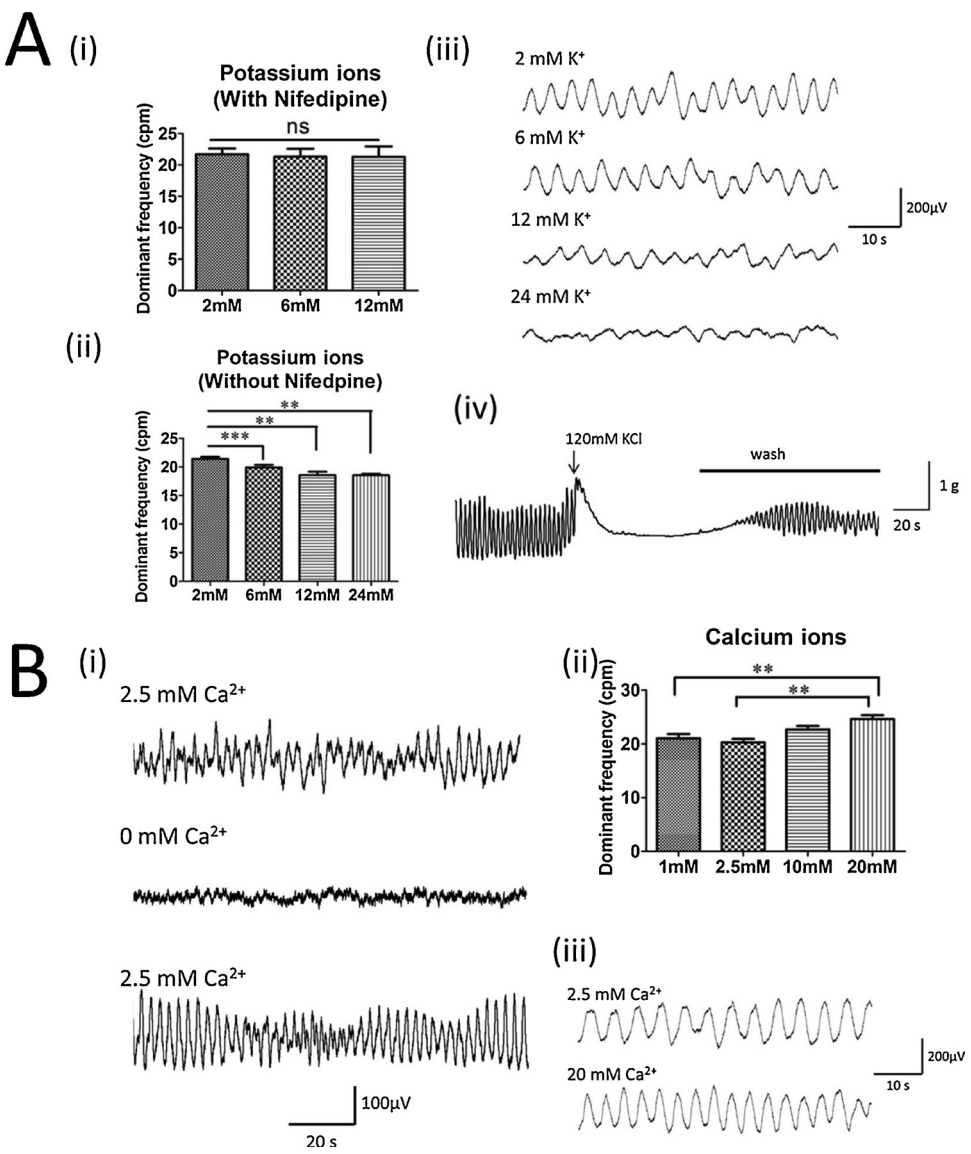

Fig. 7. The effects of different concentrations of (A) potassium (K^+) and (B) calcium (Ca^{2+}) on pacemaker frequency in the mouse ileum. **(A)** Data are the mean ± S.E.M. of 6–8 determinations **(i)** in the presence, and **(ii)** in the absence of nifedipine (1 μM). Significant differences relative to 24 mM are indicated as ** $p < 0.01$ (one-way ANOVA followed by Tukey's multiple comparison tests). Significant differences between 2 mM and 6 mM in (ii) are indicated as *** $p < 0.001$ (paired *t*-tests); **(iii)** representative raw traces showing the inhibition of pacemaker potential and frequency upon increasing potassium ion concentration in the absence of 1 μM nifedipine in the MEA; **(iv)** representative raw traces showing the addition of KCl (120 mM) led to contraction of smooth muscle in the organ bath and inhibition of spontaneous contraction, which was recovered by washing. **(B)** (i) Representative raw traces of pacemaker potential inhibition after perfusion of Krebs' without calcium ions and recovery after perfusion of Krebs' with calcium ions. **(ii)** Data are the mean ± S.E.M. of 5–6 determinations. Significant differences relative to 20 mM are indicated as ** $p < 0.01$ (one-way ANOVA followed by Tukey's multiple comparison tests); **(iii)** representative raw traces showing an increase in pacemaker frequency upon increasing calcium ion concentration from 2.5 mM to 20 mM.

pacemaker potentials generated from the point did not propagate to nearby regions. Difficulties in obtaining MEA recordings from the mouse colon could be partially explained by the physiological irregularity of smooth muscle contractions seen in the organ bath. However, these problems recording from the colon were not experienced with the *Suncus murinus* samples. Regular pacemaker activities of colon i.e. section 6 were recorded in both the MEA and the organ bath studies (Fig. 3B, 9 C).

The *Suncus murinus* model may also have other advantages over rodents. It can be used to study vomiting reflex, whereas the rodents lack this response [28]. It also has motilin receptors, which are expressed in humans, but are absent in rodents [29]. It is also likely that there might be an inter-species differences in the quality of colonic pacemaker potentials in relation to the relative sizes of the caecum. Colonic pacemaker potentials are more readily recorded form both *Suncus murinus* and ferrets (data not shown), which have a less defined caecum; whereas it is more challenging to record stable colonic pacemaker potentials from rats and mice, where they have a more defined caecum.

4.3. Temperature and tissue section dependence of pacemaker potentials

A similarity shared between the mouse and *Suncus murinus* is that the pacemaker frequency of the stomach was significantly lower than the intestine. Although this is a well-known phenomenon, cellular control of pacemaker frequencies in different GI tissues has not been elucidated. One hypothesis suggests that the density of ICCs contributes to the frequencies observed [3]. The differences in frequencies were also reflected in the spontaneous smooth muscles activities in the organ bath studies.

Upon temperature increase, the pacemaker frequency increases significantly. However, the increase in temperature affects the pacemaker frequency of the stomach only in the mouse, but not in the *Suncus murinus*. While in humans, drinking either cold or hot water increases the slow wave frequency of the stomach [30]. It is known that a variety of temperature sensitive receptors, such as the transient receptor potential receptors, TPRV1, TPRV3, TPRA1, TPRM8, are expressed along the entire GI tract in different species, including humans [31]. Profiling these receptor expressions in the mouse, *Suncus murinus* and human stomach, as well as the rest of the intestine, might help us understand the inter-species differences in pacemaker frequencies under different temperatures in different tissue sections.

Other differences in the gut physiology between the mouse and the *Suncus murinus* include a drop in frequency from the duodenum to colon observed in the mouse, but not *Suncus murinus*. This drop is also found in humans [32]. Moreover, the propagation velocity is the highest at

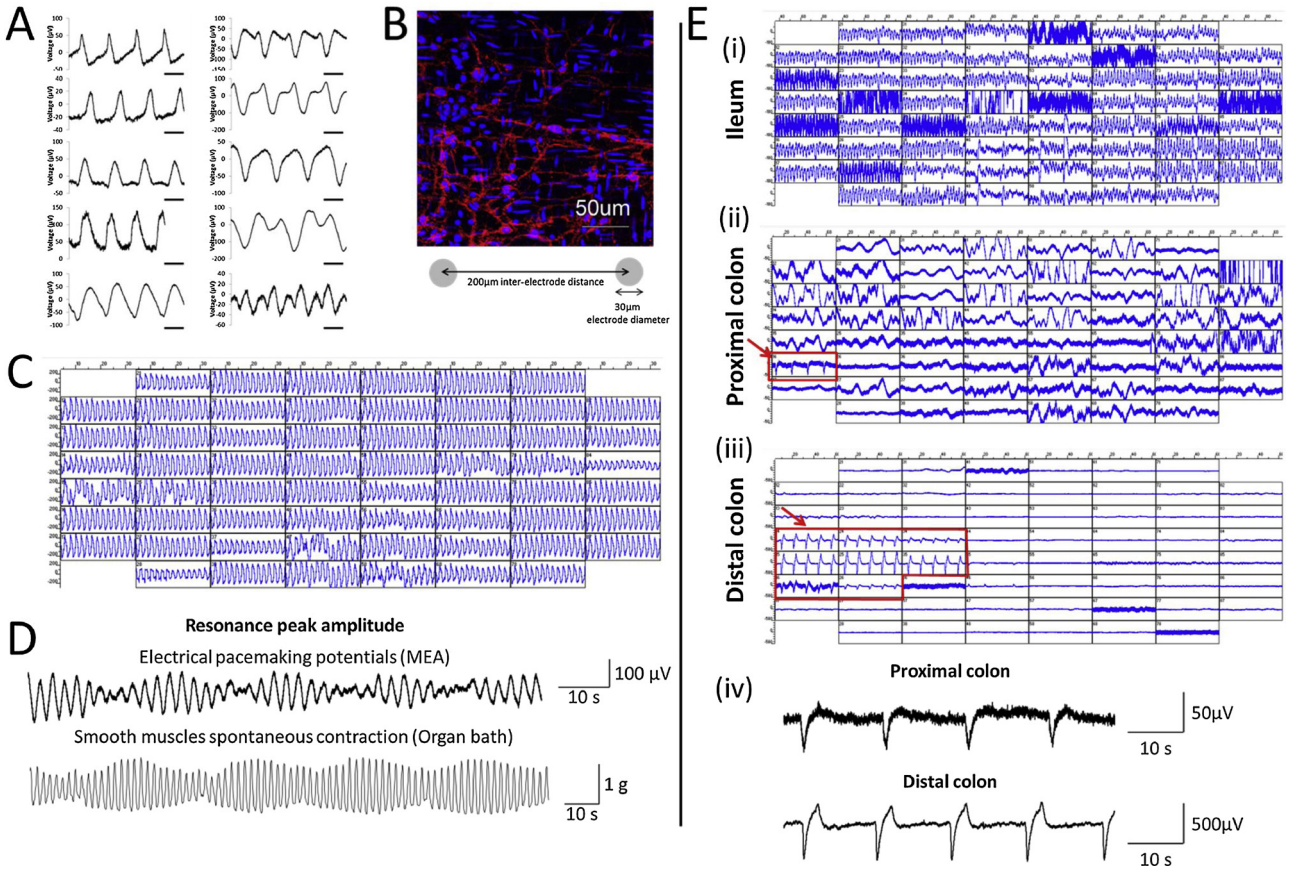

Fig. 8. Interference of recorded signals and limitations of the MEA. (A) Random selected raw traces showing differently shaped waveforms of pacemaker potentials recorded from the mouse ileum at 35 °C. Scale bar = 2 s. **(B)** Immunofluorescence staining of ICC cells in the mouse ileum. ICC cells which were c-kit^{+} are shown in red with TRITC-linked secondary antibodies; nuclei counter-stained with DAPI are shown in blue. The 3D MEA had an inter-electrode distance of 200 μm, and electrode diameter of 30 μm. The size of the MEA electrodes was constructed according to the scale bar on the immunofluorescence image. **(C)** Representative raw traces showing pacemaker potentials recorded from *Suncus murinus* synchronized in all 60 channels on the MEA. **(D)** Resonance pacemaker potentials recorded by the MEA and resonance-like smooth muscle spontaneous contractions measured by the organ bath. **(E)** Raw traces recorded from the MEA in **(i)** the ileum; **(ii)** proximal colon; and **(iii)** distal colon of the mouse; **(iv)** representative raw traces of successful recordings of pacemaker potentials from the mouse proximal and distal colon.

section 1 (duodenum) in *Suncus murinus*, whereas it is highest in the jejunum of the mouse. In humans, the highest propagation velocity has been found in the duodenum [32], similar to *Suncus murinus*. Overall, the pacemaker frequencies of the whole gut in both the mouse and *Suncus murinus* are higher than those found in the human gut [32]. The inter-species differences in the gut physiology between the mouse, *Suncus murinus*, as well as humans, are probably evolutionary and genetically based as reflected in different digestive physiology and habits. To our knowledge, no other study has investigated the function of ICCs from *Suncus murinus* and compared their physiological differences to the mouse or human. Since we have demonstrated significant inter-species variations on gut pacemaker physiology, care must be taken when attempting to translate the findings in animal models to human gut physiology.

Physiologically, the gut sensitivity towards temperature may not seem important since animal used in this manuscript are all warm-blooded, where the temperature of the gut is maintained by the body temperature. However, during ingestion, food temperature may directly influence gut motility. For example, to avoid extreme food temperatures physically damaging the surface of the gut lumen, a more frequent gut movement helps increase the surface area for dissipating heat energy. In our results, the pacemaker frequency and propagation velocity was generally higher in the proximal intestine, while the amplitude was higher in the distal end of the intestine. A higher propagation velocity and frequency in the proximal intestine may be envisaged to permit a better mixing of food with digestive juice and increases the surface area for absorption of nutrients, while a lower propagation velocity and frequency, but larger amplitude in the distal gut may allow enough time for water reabsorption and to push large fecal pellet forward. Overall, the current findings are consistent with basic gut physiology.

The pacemaker frequencies we found in the mouse are very similar to those reported in literature [33–36]. However, it is important to note that whilst our studies used intact tissues, others made recordings from ICCs in culture, or from the LMMP after the removal of mucosal layer; this may significantly reduce/alter the pacemaker frequency recorded [12,14,37,38]. In fact, the signals we recorded had a ~2-5 times higher amplitude (50-100μV for the mouse) than those previously recorded, e.g. ± 20 μV [13]; ± 25 μV in [12].

Based on previous investigations of pacemaker potential using *in-vivo* radio-telemetry techniques in ICR mice, the gastric pacemaker frequency was revealed to be 6.8 ± 0.6 cpm at a body temperature of 33.8 ± 2.4 °C [39], which is very similar to the pacemaker frequency of 6.5 ± 0.4 cpm at 35 °C in the present studies. Another study tried to use the *in-vivo* imaging technique, making use of a dye to visualize intestinal motility and found that the pacemaker frequency was 27–35 cpm in the small intestine [40], which is also very close to what we found in the small intestine using the MEA.

The findings of our study also raised an interesting question: different from whole animal study, where the peristalsis wave front may continuously propagate from the proximal end to the distal end of the

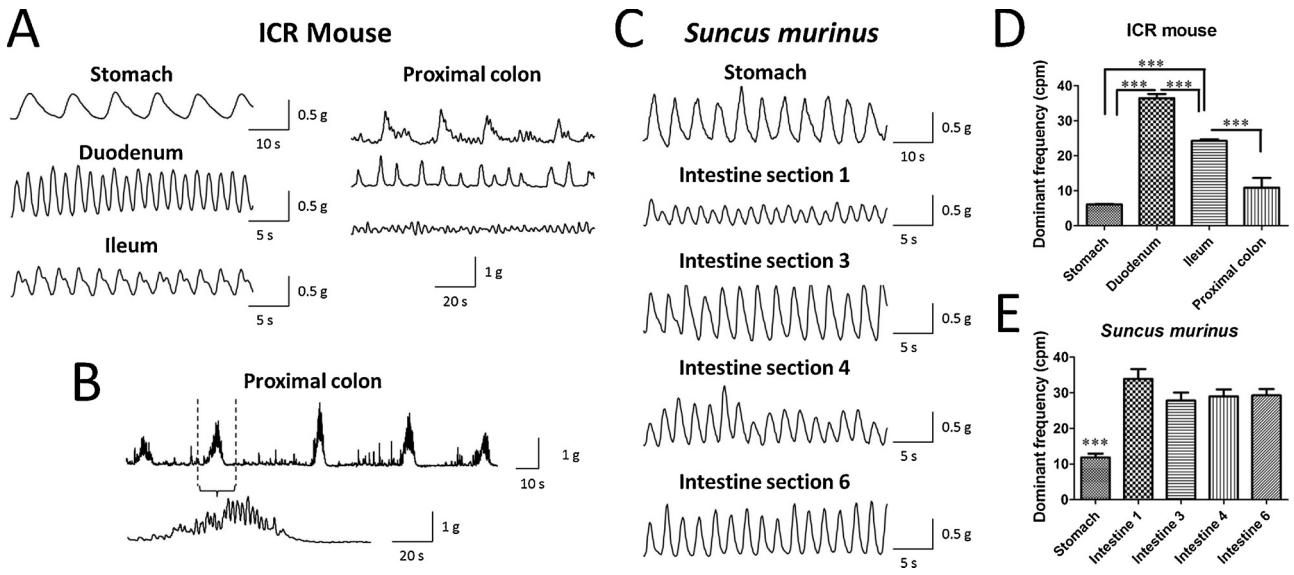

Fig. 9. Gastrointestinal smooth muscle spontaneous contractions and relaxations recorded using the organ bath set up. (A) Representative raw traces from the ICR mouse. The stomach, duodenum and ileum show regular pacemaker patterns; in contrast, the proximal colon shows a wide variety of patterns. **(B)** In some of the proximal colon samples, a migrating myoelectric complex can be observed. **(C)** Representative raw traces from *Suncus murinus*. **(D)** Data are the mean ± S.E.M. of 6–10 determinations. Significant differences are indicated as *** $p < 0.001$ (one-way ANOVA followed by Tukey's multiple comparison tests). **(E)** Data are the mean ± S.E.M. of 5–6 determinations. Significant differences between the stomach and all the intestinal sections are indicated as *** $p < 0.001$ (one-way ANOVA followed by Tukey's multiple comparison tests).

gut, we are using isolated tissues on the MEA and organ bath. How do each isolated tissue sections maintain their own pacemaker frequency and propagation velocity? The ICC cells at each tissue section are probably expressing differential regulatory machinery to control the frequency and propagation velocity, which may be interesting to look into further.

Based on previous findings [5,6,21] and the observations of the current study, GI pacemaker potentials largely depend on specific tissue sections and the incubation temperature. Care must therefore be taken to avoid the use of the general term "small intestine" without specifying the duodenum or ileum. In addition, incubating at room temperature may make comparative studies difficult [34,41]. Moreover, isolated ICCs cultured from the whole intestine may not behave consistently from cell to cell: the ICCs from the proximal intestine could behave very differently from those in the distal region and ICCs present in the submucosal plexus, myenteric plexus or within the muscular layers

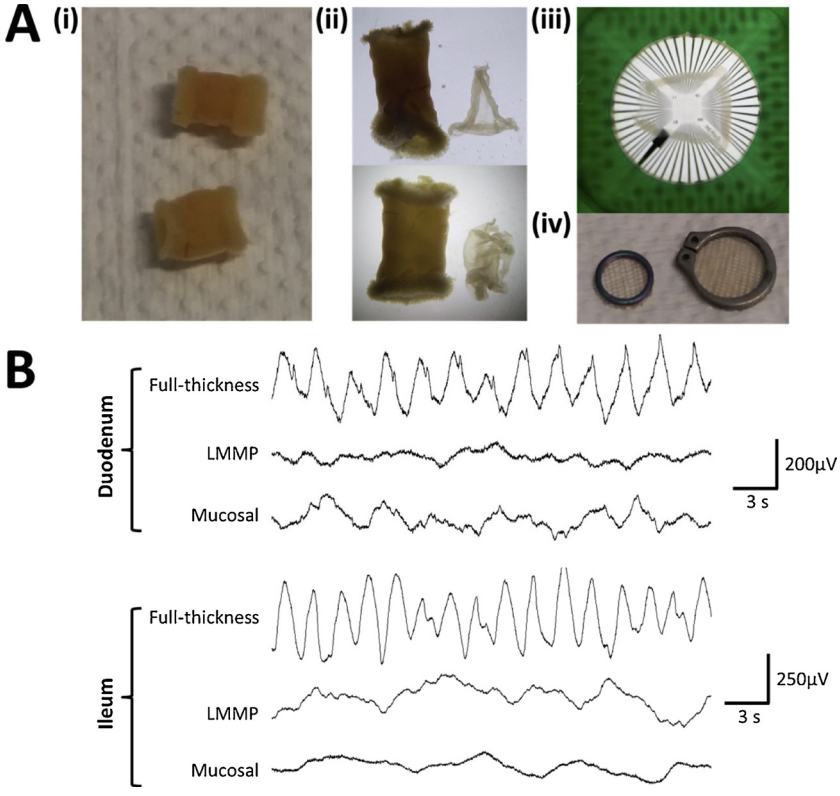

Fig. 10. Pacemaker potentials recorded from full-thickness tissues, isolated LMMP and isolated mucosal layer of the *Suncus murinus*. (A) Photographs showing (i) the appearance of a full-thickness tissues, (ii) isolated mucosal layer (left) and isolated LMMP layer (right) of the same tissue of a section of the duodenum (upper) and the ileum (lower) of tissues from *Suncus murinus*. The diameter of the each tissue is approximately 6–7 mm. (iii) The LMMP was flattened as shown onto the recording area under a dissecting microscope. (iv) Weight was added on top of the LMMP with two tissue anchors: a small anchor with diameter 0.5 mm followed by a large anchor with 0.8 mm diameter. (B) Representative raw traces of the baseline recordings using the same tissues shown in A.

could also behave differently.

4.4. Modification of the MEA technique to record GI pacemaker potentials

The MEA has been used to record GI pacemaker activities in previous studies [12–14,22]. Several studies made recordings from isolated longitudinal muscle myenteric plexus (LMMP) layers or had the mucosal layer removed physically. In this study, full-thickness tissue preparations were used that included the mucosal layer. We believe that although ICCs in the myenteric plexus are believed to play a critical role in regulating pacemaker potentials [3], a modulatory role of ICCs located in the muscular layers or submucosal plexus should not to be ignored. In our experiment, we showed that separating the LMMP and the mucosal layer severely disrupted the pacemaker signals compared with the signals obtained from a full-thickness preparation of the same tissues. This result from damage towards the coordination and synchronization of the ICC networks between the two layers. Here, it is important to note that the MEA records pacemaker signals from a network of ICCs, while the conventional microelectrode records from a single ICC cell. Loss of coordination within the ICC networks might have led to the irregularity in the signals recorded. For example, signals from uncoordinated and unsynchronized ICCs would interfere each other. Besides, the more damage done to the tissues, the less translatable the result is to the *in-vivo* situation. The procedure of peeling off the LMMP or removal of the mucosal layer has raptured most of the neuronal and cellular connections between the two layers. Separating the LMMP and mucosal layer may allow us to understand how ICCs at different layers behave, but the communication between the two layers are totally lost. For example, many sensory receptors, as well as enterochromaffin cells are restricted to the mucosal layer [42]. Upon activation, signals are transduced via hormones or neuronal connections from the mucosal layer to the muscular layer to induce a final response in gut motility. Therefore, the results generate by isolated layers may not translate to the true and final effects of a drug treatments. In particular, if we aim to use the technique for studying pharmacology, we would like observed a more complete picture, and keep connections, signal transduction, regulatory and compensatory machinery between the mucosal and muscular layers as intact as possible. The microelectrode technique procedure requires the removal of the mucosal layer as microelectrode is too fragile to insert through the thickness of the mucosal layer. However, this is not a problem when using the MEA.

We also used a lower sampling rate of 1 kHz, rather than the 20 kHz used in previous studies [12–14,22], and found that 1 kHz was sufficient to identify the pacemaker potentials. The pacemaker frequency the tissues we recorded from never exceeds 50 cpm, i.e. 0.83 Hz. Theoretically, we may use a much lower sampling rate, such as 512 Hz [9,43,44], but the lowest possible sampling rate of our MEA system was 1 kHz. Furthermore, we carefully maintained the natural state of the tissue for drug testing in subsequent studies. Integrated effects of neurons and networks of ICCs in smooth muscle and mucosal layers are expected to be important.

4.5. Nifedipine as muscle relaxant

Nifedipine, an L-type calcium ion channel blocker, has been used to paralyze smooth muscles in many studies over years [36,38,45]. A combination of nifedipine and mibefradil, a T-type calcium ions channel blocker, was found to inhibit ICC pacemaker potentials, but the effect was not observed when the drugs were administered alone [6]. Similar findings were also seen with a combination of nickel ions and nifedipine [46]. While nifedipine is used to inhibit smooth muscle contractions, the present study provides evidence that nifedipine may have secondary effects on responses to $[K^+]_o$, which could in turn alter pacemaker potentials. Care must be taken when using nifedipine as muscle relaxant to ensure its presence will not affect the final results. However, without the administration of nifedipine, movements may interfere with the contact between the MEA and the tissue sample, leading to reduced signal quality. Nifedipine may also be expected to have effects on pacemaker potentials. We believed that the simultaneous use of an organ bath to study the spontaneous contractions of smooth muscles as a final outcome of ICC pacemaker potentials would allow us to understand the role of ICC–smooth muscle coupling in GI electro-mechanics. We believed that the simultaneous use of an organ bath to study the spontaneous contractions of smooth muscles as a final outcome of ICC pacemaker potentials would allow us to understand the role of ICC–smooth muscle coupling in GI electromechanics.

4.6. Limitations of data recorded from the MEA

The amplitudes of pacemaker potentials recorded from the MEA varied from ± 20–300 μV in the presence of ± 2–10 μV noise, which translates to a signal-to-noise ratio range of 3–22 dB. This signal-to-noise ratio is low compared to those obtained using conventional single cell microelectrode [6]. This is because the amplitudes of extracellular field potentials are directly affected by the contact between the tissues and electrodes, as well as the depth of ICCs within the tissues. Besides, minor movements, such as from perfusion and trapped air bubbles, could also affect the amplitude. Single cell microelectrode recording techniques allows users to manually insert the electrode needle into a position very close to an ICC cell, but the methodology do not yield information on propagation which is useful to understanding mechanisms of dysrhythmia. In our studies, pacemaker potentials with clear waveforms and frequencies matching to the literature were readily recorded [33–36]. We believe that with correct preparation and applications of filters, the MEA is sufficient in its sensitivity to detecting the frequency changes, as demonstrated by several studies [10,47,48]. Moreover, the MEA certainly also has advantages over the single cell microelectrode, where it can simultaneously record from an array of electrodes to provide information on the temporal profile and its spatial function.

The waveform of extracellular field potentials can also be affected by numerous factors: (1) interference from unsynchronized populations of ICCs; (2) interference from other electrically active cells or receptors' ion channels; and (3) incomplete inhibition of smooth muscle activity. The interference from (2) can be minimized by using a sampling frequency of 1 kHz, as discussed previously; while interference from (3) can be minimized by using nifedipine (1 μM), which is effective within 1–2 min as revealed by the organ bath study (data not shown). However, interference from (1) can produce significant variations in the waveforms (Fig. 8A,D), with a lag between pacemaker potentials within different portions of the MEA, while the pacemaker frequency is consistent. Given that such interference is unavoidable, it is difficult to draw firm conclusions relating to the amplitude and waveform activity of the slow waves across different preparations. However, pacemaker frequency and propagation velocity appear to be less affected by interference, suggesting that the MEA recording technique could be used to investigate the effects of different drug treatments on slow wave networking.

4.7. Differences between the pacemaker frequency obtained from the organ bath and the MEA

The pacemaker frequency obtained in the organ bath is also different from the MEA in our study. In the stomach, the frequency is higher measured by the MEA than the organ bath in the mouse, but is lower in the *Suncus murinus*. In the intestine, the frequency is higher measured by the organ bath than the MEA in both the mouse and *Suncus murinus*. This difference could be explained by the stretch applied to the tissues in the organ bath to provide enough tension to measure the smooth muscles contractions by the isometric force displacement transducer. This procedure may activate mechanosensitive

receptors, while the tissues are not under tension in recordings made from the MEA. Another possible reason is the involvement of smooth muscles in modulating pacemaker frequency which may be blocked by nifedipine treatment to inhibit movements on the MEA.

Declarations of interest

None.

Conflict of interest

The authors declare that there is no conflict of interest.

Financial support

This research did not receive any specific grant from funding agencies in the public, commercial, or not-for-profit sectors.

Author contributions

Julia Y. H. Liu and John A. Rudd designed the experiment. Julia Y. H. Liu performed the experiment and analyzed the data. Peng Du designed the mathematical algorithm for the spatiotemporal analysis of the wave propagation data. Julia Y. H. Liu, Peng Du, W. Y. Chan and John A. Rudd wrote the manuscript.

Acknowledgments

We greatly appreciate the Spike 2 script provided by Simon Gray from Cambridge Electronic Design Limited.

References

[1] K.M. Sanders, S.D. Koh, S.M. Ward, Interstitial cells of cajal as pacemakers in the gastrointestinal tract, Annu. Rev. Physiol. 68 (2006) 307–343.
[2] J.D. Huizinga, S. Martz, V. Gil, X.Y. Wang, M. Jimenez, S. Parsons, Two independent networks of interstitial cells of cajal work cooperatively with the enteric nervous system to create colonic motor patterns, Front. Neurosci. 5 (2011) 93.
[3] O.A. Al-Shboul, The importance of interstitial cells of cajal in the gastrointestinal tract, Saudi J. Gastroenterol. 19 (2013) 3–15.
[4] A.J. Burns, Disorders of interstitial cells of Cajal, J. Pediatr. Gastroenterol. Nutr. 45 (Suppl 2) (2007) S103–106.
[5] Y. Kito, H. Suzuki, Effects of temperature on pacemaker potentials in the mouse small intestine, Pflugers Arch. 454 (2007) 263–275.
[6] A. Hotta, N. Okada, H. Suzuki, Mibefradil-sensitive component involved in the plateau potential in submucosal interstitial cells of the murine proximal colon, Biochem. Biophys. Res. Commun. 353 (2007) 170–176.
[7] H. Zheng, K.S. Park, S.D. Koh, K.M. Sanders, Expression and function of a T-type Ca2+ conductance in interstitial cells of Cajal of the murine small intestine, American journal of physiology, Cell Physiol. 306 (2014) C705–713.
[8] G. O'Grady, T.L. Abell, Gastric arrhythmias in gastroparesis: low- and high-resolution mapping of gastric electrical activity, Gastroenterol. Clin. North Am. 44 (2015) 169–184.
[9] T.R. Angeli, P. Du, N. Paskaranandavadivel, S. Sathar, A. Hall, S.J. Asirvatham, G. Farrugia, J.A. Windsor, L.K. Cheng, G. O'Grady, High-resolution electrical mapping of porcine gastric slow-wave propagation from the mucosal surface, Neurogastroenterol. Motil. 29 (2017).
[10] N. Paskaranandavadivel, L.K. Cheng, P. Du, J.M. Rogers, G. O'Grady, High-resolution mapping of gastric slow-wave recovery profiles: biophysical model, methodology, and demonstration of applications, Am. J. Physiol. Gastrointestinal Liver Physiol. 313 (2017) G265–G276.
[11] J. Putney, G. O'Grady, T.R. Angeli, N. Paskaranandavadivel, L.K. Cheng, J.C. Erickson, D. Peng, Determining the efficient inter-electrode distance for high-resolution mapping using a mathematical model of human gastric dysrhythmias, Conference Proceedings : … Annual International Conference of the IEEE Engineering in Medicine and Biology Society. IEEE Engineering in Medicine and Biology Society. Annual Conference, 2015, (2015), pp. 1448–1451.
[12] H.N. Liu, S. Ohya, Y. Nishizawa, K. Sawamura, S. Iino, M.M. Syed, K. Goto, Y. Imaizumi, S. Nakayama, Serotonin augments gut pacemaker activity via 5-HT3 receptors, PLoS One 6 (2011) e24928.
[13] S. Nakayama, R. Ohishi, K. Sawamura, K. Watanabe, K. Hirose, Microelectrode array evaluation of gut pacemaker activity in wild-type and W/W(v) mice, Biosens. Bioelectron. 25 (2009) 61–67.
[14] H.B. Shozib, H. Suzuki, S. Iino, S. Nakayama, Acceleration of ileal pacemaker activity in mice lacking interleukin 10, Inflamm. Bowel Dis. 19 (2013) 1577–1585.
[15] O. Bayguinov, G.W. Hennig, K.M. Sanders, Movement based artifacts may contaminate extracellular electrical recordings from GI muscles, Neurogastroenterol. Motil. 23 (2011) 1029–1042 e1498.
[16] K. Kuroda, H. Hequing, A. Mondal, M. Yoshimura, K. Ito, T. Mikami, S. Takemi, T. Jogahara, I. Sakata, T. Sakai, Ghrelin is an essential factor for motilin-induced gastric contraction in Suncus murinus, Endocrinology 156 (2015) 4437–4447.
[17] V. Georgiadis, A. Stephanou, P.A. Townsend, T.R. Jackson, MultiElec: a MATLAB based application for MEA data analysis, PLoS One 10 (2015) e0129389.
[18] R. Yassi, G. O'Grady, N. Paskaranandavadivel, P. Du, T.R. Angeli, A.J. Pullan, L.K. Cheng, J.C. Erickson, The gastrointestinal electrical mapping suite (GEMS): software for analyzing and visualizing high-resolution (multi-electrode) recordings in spatiotemporal detail, BMC Gastroenterol. 12 (2012) 60.
[19] J.C. Erickson, G. O'Grady, P. Du, C. Obioha, W. Qiao, W.O. Richards, L.A. Bradshaw, A.J. Pullan, L.K. Cheng, Falling-edge, variable threshold (FEVT) method for the automated detection of gastric slow wave events in high-resolution serosal electrode recordings, Ann. Biomed. Eng. 38 (2010) 1511–1529.
[20] P.V. Bayly, B.H. KenKnight, J.M. Rogers, E.E. Johnson, R.E. Ideker, W.M. Smith, Spatial organization, predictability, and determinism in ventricular fibrillation, Chaos 8 (1998) 103–115.
[21] P. Langton, S.M. Ward, A. Carl, M.A. Norell, K.M. Sanders, Spontaneous electrical activity of interstitial cells of Cajal isolated from canine proximal colon, Proc. Natl. Acad. Sci. U.S.A. 86 (1989) 7280–7284.
[22] N. Iwata, T. Fujimura, C. Takai, K. Odani, S. Kawano, S. Nakayama, Dialysis membrane-enforced microelectrode array measurement of diverse gut electrical activity, Biosens. Bioelectron. 94 (2017) 312–320.
[23] H. Koshiba, [Comparison of drug effects on the isolated rat colon and duodenum], Nihon yakurigaku zasshi, Folia Pharmacol. Jpn. 71 (1975) 415–426.
[24] A.M. Martin, A.L. Lumsden, R.L. Young, C.F. Jessup, N.J. Spencer, D.J. Keating, The nutrient-sensing repertoires of mouse enterochromaffin cells differ between duodenum and colon, Neurogastroenterol. Motil. 29 (2017).
[25] A. Samson, K.L. Hamilton, A.G. Butt, Effect of somatostatin on electrogenic ion transport in the duodenum and colon of the mouse, Mus domesticus, Compar. Biochem. Physiol. Part A Mol. Integr. Physiol. 125 (2000) 459–468.
[26] K.M. Sanders, S.M. Ward, Interstitial cells of Cajal: a new perspective on smooth muscle function, J. Physiol. (Lond.) 576 (2006) 721–726.
[27] B. Alberts, A. Johnson, J. Lewis, Ion Channels and the Electrical Properties of Membranes, Molecular Biology of the Cell, 4th edition, Garland Science, New York, 2002.
[28] C.C. Horn, B.A. Kimball, H. Wang, J. Kaus, S. Dienel, A. Nagy, G.R. Gathright, B.J. Yates, P.L. Andrews, Why can't rodents vomit? A comparative behavioral, anatomical, and physiological study, PLoS One 8 (2013) e60537.
[29] J. He, D.M. Irwin, R. Chen, Y.P. Zhang, Stepwise loss of motilin and its specific receptor genes in rodents, J. Mol. Endocrinol. 44 (2010) 37–44.
[30] W.M. Sun, R. Penagini, G. Hebbard, C. Malbert, K.L. Jones, S. Emery, J. Dent, M. Horowitz, Effect of drink temperature on antropyloroduodenal motility and gastric electrical activity in humans, Gut 37 (1995) 329–334.
[31] P. Holzer, TRP channels in the digestive system, Curr. Pharm. Biotechnol. 12 (2011) 24–34.
[32] A.S. Lin, M.L. Buist, N.P. Smith, A.J. Pullan, Modelling slow wave activity in the small intestine, J. Theor. Biol. 242 (2006) 356–362.
[33] A.S. Forrest, G.W. Hennig, S. Jokela-Willis, C.D. Park, K.M. Sanders, Prostaglandin regulation of gastric slow waves and peristalsis, Am. J. Physiol. Gastrointestinal Liver Physiol. 296 (2009) G1180–1190.
[34] Y. Kito, H. Suzuki, Properties of pacemaker potentials recorded from myenteric interstitial cells of Cajal distributed in the mouse small intestine, J. Physiol. (Lond.) 553 (2003) 803–818.
[35] N.J. Spencer, K.M. Sanders, T.K. Smith, Migrating motor complexes do not require electrical slow waves in the mouse small intestine, J. Physiol. (Lond.) 553 (2003) 881–893.
[36] A.A. Worth, A.S. Forrest, L.E. Peri, S.M. Ward, G.W. Hennig, K.M. Sanders, Regulation of gastric electrical and mechanical activity by cholinesterases in mice, J. Neurogastroenterol. Motil. 21 (2015) 200–216.
[37] S.D. Koh, J.Y. Jun, T.W. Kim, K.M. Sanders, A Ca(2+)-inhibited non-selective cation conductance contributes to pacemaker currents in mouse interstitial cell of Cajal, J. Physiol. (Lond.) 540 (2002) 803–814.
[38] S.D. Koh, T.W. Kim, J.Y. Jun, N.J. Glasgow, S.M. Ward, K.M. Sanders, Regulation of pacemaker currents in interstitial cells of Cajal from murine small intestine by cyclic nucleotides, J. Physiol. (Lond.) 527 (Pt 1) (2000) 149–162.
[39] H. Wang, Z. Lu, Y.H. Liu, Y. Sun, L. Tu, M.P. Ngan, C.K. Yeung, J.A. Rudd, Establishment of a radiotelemetric recording technique in mice to investigate gastric slow waves: modulatory role of putative neurotransmitter systems, Exp. Physiol. 103 (2018) 827–837.
[40] S. Kwon, E.M. Sevick-Muraca, Non-invasive, dynamic imaging of murine intestinal motility, Neurogastroenterol. Motil. 23 (2011) 881–e344.
[41] Y. Cai, H. Tang, F. Jiang, Z. Dong, Slow wave activity and modulations in mouse jejunum myenteric plexus in situ, J. Neurogastroenterol. Motil. 23 (2017) 117–123.
[42] A.R. Gunawardene, B.M. Corfe, C.A. Staton, Classification and functions of enteroendocrine cells of the lower gastrointestinal tract, Int. J. Exp. Pathol. 92 (2011) 219–231.
[43] P. Du, G. O'Grady, J.U. Egbuji, W.J. Lammers, D. Budgett, P. Nielsen, J.A. Windsor, A.J. Pullan, L.K. Cheng, High-resolution mapping of in vivo gastrointestinal slow wave activity using flexible printed circuit board electrodes: methodology and validation, Ann. Biomed. Eng. 37 (2009) 839–846.
[44] E.J. Lutton, W. Lammers, S. James, H.A. van den Berg, A.M. Blanks, Identification of uterine pacemaker regions at the myometrial-placental interface in the rat, J. Physiol. (Lond.) 596 (2018) 2841–2852.

[45] S.M. Ward, S.C. Harney, J.R. Bayguinov, G.J. McLaren, K.M. Sanders, Development of electrical rhythmicity in the murine gastrointestinal tract is specifically encoded in the tunica muscularis, J. Physiol. (Lond.) 505 (Pt 1) (1997) 241–258.
[46] S.M. Ward, K.M. Sanders, Dependence of electrical slow waves of canine colonic smooth muscle on calcium gradient, J. Physiol. (Lond.) 455 (1992) 307–319.
[47] G. O'Grady, T. Angeli, P. Du, L.K. Cheng, Concerning the validity of gastrointestinal extracellular recordings, Physiol. Rev. 95 (2015) 691–692.
[48] N. Paskaranandavadivel, G. O'Grady, P. Du, L.K. Cheng, Comparison of filtering methods for extracellular gastric slow wave recordings, Neurogastroenterol. Motil. 25 (2013) 79–83.